Chaos, Solitons & Fractals 50 (2013) 39–47

Contents lists available at SciVerse ScienceDirect

Chaos, Solitons & Fractals

Nonlinear Science, and Nonequilibrium and Complex Phenomena

journal homepage: www.elsevier.com/locate/chaos

Modelling a molecular calendar: The seasonal photoperiodic response in mammals

Oliver Ebenhöh [a], David Hazlerigg [b,*]

[a] Institute of Complex Systems and Mathematical Biology, University of Aberdeen, Scotland, UK
[b] Institute of Biological and Environmental Sciences, University of Aberdeen, Scotland, UK

ARTICLE INFO

Article history:
Available online 21 December 2012

ABSTRACT

Organisms use biological timing mechanisms to synchronise life-history transitions to annual environmental cycles. For species living outside the equatorial zone, day length change is a widely used external cue for seasonal biological clocks. This paper builds on recent developments in understanding the neuroanatomical basis of day length measurement (photoperiodism) in mammals, by taking a modelling approach to the molecular readout mechanism. We find that, while a circadian clock based system can drive day length dependent changes in the amplitude of a seasonal output (in this case production of the hormone thyrotrophin), the inclusion of a positive feedback based amplifier mechanism generates photoperiodic transitions that more closely match experimental observations. The analogies between our model and those proposed for boundary generation in developmental biology are briefly discussed.

1. Introduction

Across taxa, seasonal life history transitions are a fundamental property of life, essential for Darwinian fitness. Two key features of these transitions are (1) – that they are generally *transitory* because intermediate states (e.g. partially feather moulted, or partially reproductively active) are costly, and (2) – that synchronisation of these transitions to the environmental seasons often relies upon day length (photoperiod), as the most reliable indicator of forthcoming seasonal changes.

In a laboratory setting it is possible to simulate seasonal responses to environmental photoperiod by using controlled lighting regimes, and to exploit these to explore the underlying mechanisms of photoperiodic synchronization. Classical work in this area demonstrates firstly that photoperiodic time measurement relies upon circadian clocks and secondly that transitions in physiological status in the lab typically occur when day length exceeds (or falls below, for autumn driven phenomena) a certain Critical Day-length [1]. Bünning hypothesised that the same circadian clocks underlying daily rhythms of behaviour were also responsible for photoperiodic time-measurement, and he advanced the notion of External Coincidence timing to account for circadian clock involvement [2] (Fig. 1A). According to his model, the circadian clock generates a rhythm of sensitivity to light, with maximum light sensitivity (the so-called photoinducible phase, ϕ_i) occurring when the internal clock predicts darkness under short photoperiods. According to this scheme a spring-like response is triggered when day length increases to the extent that (external) light exposure occurs during the photoinducible phase.

In a mammalian context, this circadian based, photoperiodic timer concept is exemplified beautifully by studies in the male Golden Hamster by Elliott (Fig. 1B), a model chosen partly because of the pronounced seasonal reproductive activity of this species, and partly because responsive variable (testicular size) can easily be assayed using a pair of calipers. Studies of the type conducted by Elliott [3] and others are generally consistent with the formal concept of a circadian external coincidence timing mechanism

* Corresponding author.
E-mail addresses: ebenhoeh@abdn.ac.uk (O. Ebenhöh), d.hazlerigg@abdn.ac.uk (D. Hazlerigg).

0960-0779
http://dx.doi.org/10.1016/j.chaos.2012.11.007

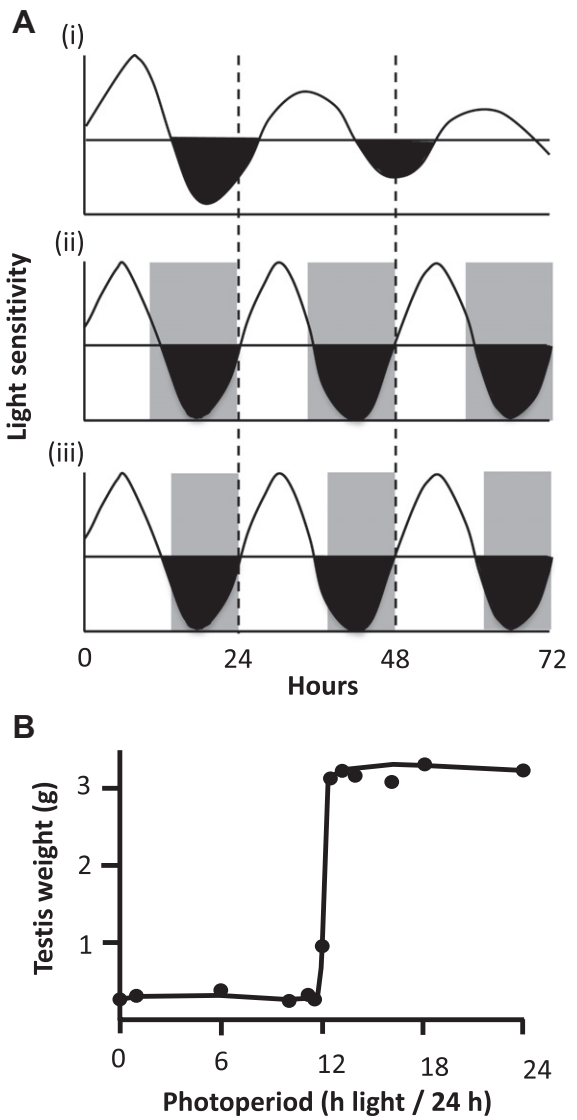

Fig. 1. A. An external coincidence timing model for photoperiodic time measurement. (i) The model, after [2] and references therein, postulates the existence of a circadian rhythm of light sensitivity, which continues when the organism is placed in constant conditions. This rhythm includes phases when the oscillator anticipates light exposure (“subjective day”, white areas) and phases where darkness is predicted (“subjective night”, black areas). The organism’s photoperiodic response is sensitive to light exposure in this “subjective night” phase. (ii) Under short photoperiods (SP), the circadian oscillation of light sensitivity becomes entrained to the light–dark cycle such that daily light exposure only occurs during the “subjective day”, and short day type photoperiodic responses ensue (iii) By contrast, under summer long photoperiods (LP) light extends into the “subjective night” coinciding with the photoinducible phase (Φi) of the endogenous oscillator, and a long-day type photoperiodic response ensues. B. Gonadal development in hamsters raised on photoperiods from 0 to 24 h duration. Note the dramatic transition from a repressed, winter-like pattern of development to stimulated summer-like development at a photoperiod slightly exceeding 12 h duration – the so-called “critical photoperiod”, graph drawn from data in [3].

underlying mammalian seasonal synchronisation, but leave the black box of underlying biological mechanism unopened.

In the last decade our understanding of the neuroanatomical and molecular pathways involved in the seasonal reproductive response in mammals has progressed considerably [4], and it is now timely to revisit the classical formalisms of External Coincidence timing, and to assess their correspondence to modern physiological understanding. Fig. 2 summarises the regulatory pathway, derived from studies in seasonal rodents (mice, hamsters and most recently voles [5]) and ungulates (principally the sheep), and now thought to represent a fundamentally conserved mechanism in mammals.

The essential features of this pathway are as follows:

1. Light information arrives via the retina, and acts to synchronise a circadian clock in the hypothalamic suprachiasmatic nuclei (SCN)
2. The SCN control production of the neurohormone, melatonin by the pineal gland, with melatonin synthesis and secretion being high throughout the night and suppressed throughout the day. This profile of melatonin secretion is sensitive to day length, so that the longest nocturnal periods of melatonin secretion occur in winter and the shortest in summer. This photoperiodically sensitive secretion of melatonin is essential for photoperiodic synchronisation: in short, melatonin signal duration is a continuous variable proportional to the length of the night.
3. Melatonin acts through high affinity, G-protein coupled receptors located in thyrotroph cells in the pars tuberalis (PT) of the pituitary, controlling the production of the hormone, thyrotrophin (TSH), so that levels are high on long photoperiods and low under short photoperiods.
4. TSH acts through TSH-receptor expressing cells located in the basal hypothalamus to modulate processing and biological activity of thyroid hormones in this tissue – in turn controlling the pattern of release of the hypothalamic hormone governing the reproductive axis (Gonadotrophin releasing hormone, GnRH) (the details of the link between TH and GnRH release remain unclear).
5. Additionally TSH-receptors are found on the PT thyrotroph cells themselves, and it has been suggested that this may reflect a positive feedback based amplifier system to augment TSH production under permissive photoperiod.

Although the nomenclature and anatomy are probably as daunting to mathematicians as mathematics is to most biologists, it should be reasonably clear that the interpretation of the melatonin signal in the PT is key to the whole process. In this tissue, an input signal (melatonin), showing a graded change in duration over the course of the year, is transduced into an output (TSH) whose amplitude undergoes a step change as the critical day-length threshold is crossed. Hence it would appear that the mammalian external coincidence timer resides in the PT.

The molecular basis of circadian rhythm generation in mammals has been dissected in detail through the power of mouse genetics [6]. A (grossly) simplified scheme for the mammalian molecular clockwork is shown in Fig. 3A, and comprises interlocked transcription/transla-

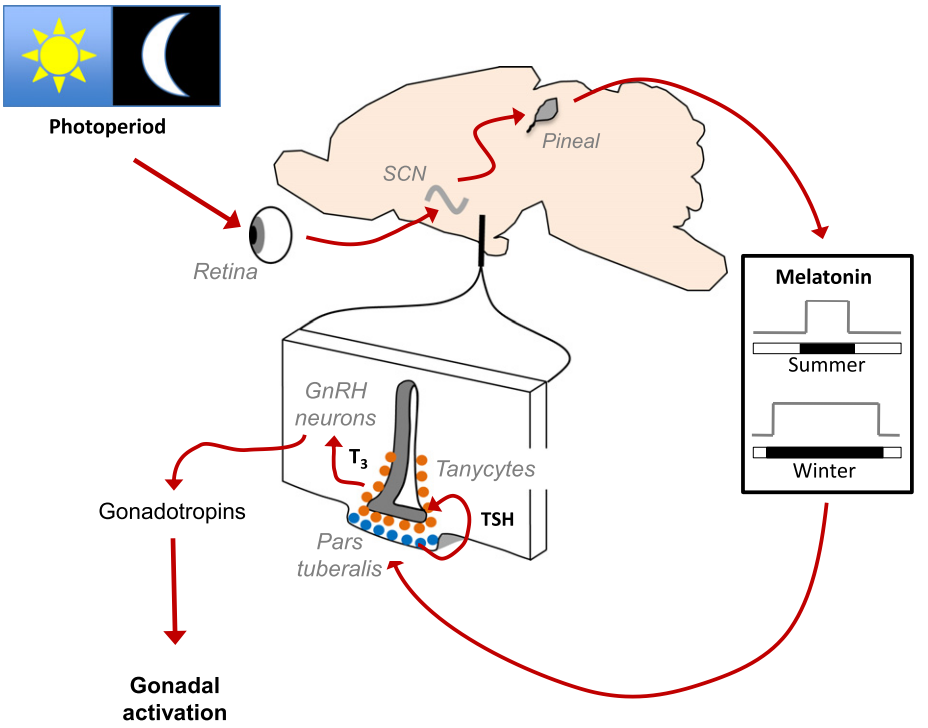

Fig. 2. Schematic model of the neuroanatomical pathway linking day light exposure to photoperiodic control of physiology in mammals. Light perceived by the retina entrains a brain circadian pacemaker residing in the suprachiasmatic nuclei (SCN) of the hypothalamus. An output of this pacemaker is the rhythmic control of melatonin synthesis by the pineal gland, producing an approximately square wave output signal in which melatonin levels are continuously high during the night and continuously low during the day. Melatonin is a hormonal signal and reaches sensitive cells in the PT region of the pituitary gland, which respond by producing a second hormonal signal, thyrotrophin (TSH) at levels reflecting the duration of the nightly melatonin signal. TSH acts in hypothalamic areas responsible with the control of seasonal physiology, such as the production of hormones controlling breeding (gonadotrophins), ultimately driving day length dependent changes in seasonal physiology.

tion feedback loops centred on a canonical group of proteins that regulate transcription through genetic response elements known as E-boxes, D-boxes and retinoid-related elements (RREs). The genes encoding these regulatory proteins are also subject to control through these elements, forming the feedback loops seemingly essential for circadian oscillation. In theory, different complements of genetic response element within the regulatory region of a given gene will set the phase of its circadian oscillation, so that complex transcriptional profiles of circadian gene expression emerge from combinatorial control by a relatively small number of canonical clock genes [7].

Viewed from the perspective of photoperiodic time-measurement, an interesting possibility is that melatonin's influences on circadian transcriptional control somehow lead to the observed amplitude regulation of TSH production by the PT. To explore this, we have examined the promoter organisation of the gene encoding the TSHβ subunit (this being rate-limiting for TSH protein biosynthesis) for the presence of E-boxes, D-boxes or RREs [8]. This revealed a functional D-box close to the transcriptional start site of the TSHβ gene, but no nearby E-boxes or RREs. Hence melatonin influences through D-box transcription became our primary candidate for involvement in a PT coincidence timing mechanism.

To explore this further, seasonally photoperiodic sheep were subjected to a transition from a regime of 8-h light/day to a regime of 16-h light/day (i.e. a transition across the critical photoperiod, achieved by delaying the timing of lights out in light controlled barns), and the profiles of RNA expression for TSHβ and a range of candidate regulators of D-box transcription were assayed in tissue samples taken every 4-h throughout the 24-h cycle on the day before the photoperiod switch and days 3 and 15 after the switch [8], (Fig. 3B). This analysis revealed that while the phase of rhythmic expression of 3 known activators of D-box transcription (Tef, Dbp and Hlf) was determined by the phase of dark onset, no day-length dependent effects on overall mean levels of expression occurred. Contrastingly, the expression of a "transcriptional coactivator", Eya3, which potently enhances D-box transcription mediated by TEF, showed a pronounced 24-h rhythm of expression peaking approximately 12.5-h after dark/melatonin onset. This phasing of the Eya3 expression rhythm means that under short photoperiods Eya3 peaks in the late night, whereas under long photoperiods it peaks in the early light phase. Strikingly, the amplitude of peak Eya3 expression is markedly higher under long photoperiod, suggesting that photoperiodic modulation of Eya3 expression lies at the core of the PT coincidence timer. A remarkably similar result was also reported recently for studies in mice [9].

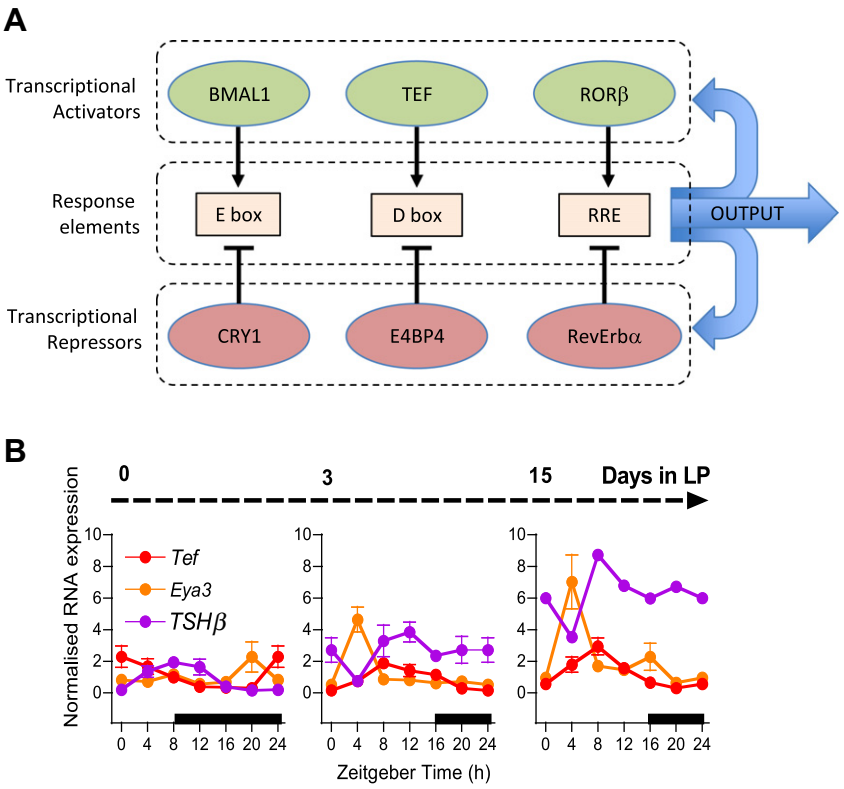

Fig. 3. A. Grossly simplified model for the generation of circadian rhythms of gene expression through coupled feedback loops. Three DNA response elements present in the promoters of rhythmically expressed genes are E boxes, D boxes and retionoid response elements (RREs) (rectangular boxes). These are governed by combinations of transcriptional regulators: activators (green elipses) exemplified by BMAL1, TEF and RORβ, and transcriptional repressors (maroon elipses), exemplified by CRY1, E4BP4 and RevErbα. Expression levels of individual genes over time (OUTPUT) are dictated by which of the different response elements are present in the promoter of that gene and the change in time in the levels of transcriptional regulators interacting with these elements. Hence a gene dominantly controlled by E boxes will show a different phasing of peak expression to a gene dominantly controlled by RREs. Cyclical expression of the transcriptional activators and repressors themselves derives from their own sensitivity to regulation through the core clock response elements, generating coupled feedback cycles of transcriptional control. For further discussion of this type of model see [7]. B. Rhythmical gene expression in the PT in response to a step increase in photoperiod. Sheep were held on an 8 h day for 8 weeks prior to a step change to 16 h light/day (LP) on Day 0, effected by delaying lights-off by 8 h (solid bars on the x axes indicate the dark phase). RNA expression profiles derived form tissue samples taken at 4 h intervals are shown for the clock gene Tef, an E box regulated, clock controlled gene, Eya3 (see text for details) and the seasonal output gene TSHβ are shown. Note how the profiles of these 3 genes respond differently at 0, 3 and 15 days of LP exposure. Further details of the study can be found in [8].

Two further observations also inform the modelling work discussed below. Firstly, in the PT, the RNA expression of Cry1, a potent repressor of E-box driven transcription, is directly induced by the nocturnal rise in melatonin, declining again within the next few hours [10]. Secondly, the promoter region of the Eya3 gene contains a functional E-box, through which transcriptional repression by CRY1 protein can take place [8].

2. Coincidence timer model

We developed a mathematical model to describe the generation of seasonal phenotypes through variations in the length of the photoperiods. The purpose of this model is to elucidate the principle mechanisms underlying seasonal responses resulting from changes in day-length, such as those observed in sheep (see above). The interactions in the model are all based on experimental findings. While for some interactions direct evidence exists, others are supported by indirect observations and the precise molecular basis remains unclear. Currently, knowledge of rate parameters and quantitative levels of mRNAs and proteins is almost non-existent. Thus, instead of attempting the impossible task of generating a validated quantitative model, our focus rather lies on the exploration of the fundamental design principles underlying the generation of seasonal responses, and as a consequence the values of the variables are all arbitrary units and only the relative changes can be interpreted in a meaningful way.

The model is schematically depicted in Fig. 4. The general idea to generate season-dependent phenotypes is based on two fundamental mechanisms. First, a coincidence timer leads to a day-length dependent expression of an output gene (here Eya3), which, secondly, exhibits a positive feedback on its own expression to stabilise the protein levels. The model generates two different phenotypes through the coexistence of two stable states (bistability), between which switching occurs as a result of changes in the environmental conditions, in our case the

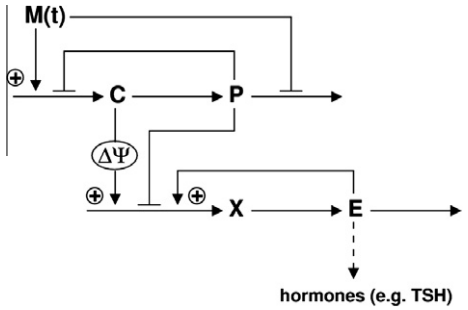

Fig. 4. Schematic representation of the interactions considered in the mathematical model. M(t) is the time-dependent melatonin level which functions as a sensor of the photoperiod. This is set to be 1 in darkness and 0 in light. Cry mRNA and protein are represented by C and P, respectively, and Eya3 mRNA and protein by X and E, respectively. Blunted headed arrows indicate inhibitory interactions, and triangular headed arrows indicate stimulatory interactions. $\Delta\Psi$ indicates a time delay. The mathematical equations and the parameters used for the calculations presented here are given in Appendix A.

day-length. Thus, the model is conceptually similar to other models studying switching behaviour in biological systems, such as signalling pathways [11] or biochemical reaction systems [12], which are all based on a positive feedback mechanism. In [12] it was recognised that such a positive feedback is indeed a necessary requirement for the generation of a bistable switch.

In the following, we describe the model in general terms and motivate the model assumptions by the existing experimental evidence. The precise mathematical formulation and the chosen parameters are described in Appendix A.

The external sensing of light is mediated by melatonin, which acts as a sensor of light/dark, being present during the night and absent during the dark. In the model, this is represented as an external, time-dependent function $M(t)$ (see Fig. 4) which equals 1 during the night and 0 during the day. Based on the evidence for direct melatonin control [10], the synthesis of Cry1 mRNA (C in the model), is modelled as being directly proportional to the function $M(t)$. Cry1 mRNA is translated into CRY1 protein (P), which inhibits the expression of Cry1. This negative feedback leads to a short peak of Cry1 expression after onset of dark. The model assumes that melatonin suppresses CRY1 protein degradation, resulting in high levels of CRY1 protein during the night and low levels during the day.

The coincidence timer exploits this mechanism by triggering the expression of the Eya3 mRNA (X in the model) at a fixed time after dusk and inhibiting Eya3 expression by CRY1-protein. Thus, in long days the trigger coincides with low levels of CRY1 protein, leading to high transcription rates of Eya3, whereas in short days the trigger meets high CRY1 protein levels, resulting in low transcription rates. Introducing a fixed trigger after dusk is motivated by RNA expression profiling studies in the PT [8,9] which demonstrate that the peak of expression of many genes in the PT is phase-locked to dark onset. Furthermore, studies from Ueda and colleagues [7] illustrate how in principle, by the correct combination of activating and inhibiting promoter elements, a gene can be constructed which peaks at any given time of the day. In our model, we use the diurnal profile of C as an indicator of the phase of the clock and simulate the expression of an output gene (here Eya3) as being activated by C with a certain phase delay ($\Delta\Psi$) relative to dark onset.

The model proposes that the coincidence-timer triggered activation of Eya3 mRNA transcription is further amplified by a positive feedback of EYA3 protein (E) on its own transcription. In the model, we implement this positive feedback as a direct activation of Eya3 transcription by EYA3 protein. Direct evidence for this molecular mechanism is based on the presence of a functional, EYA3 sensitive D box in the promoter of the Eya3 gene [8]. More generally, positive feedback amplification is also an attri-

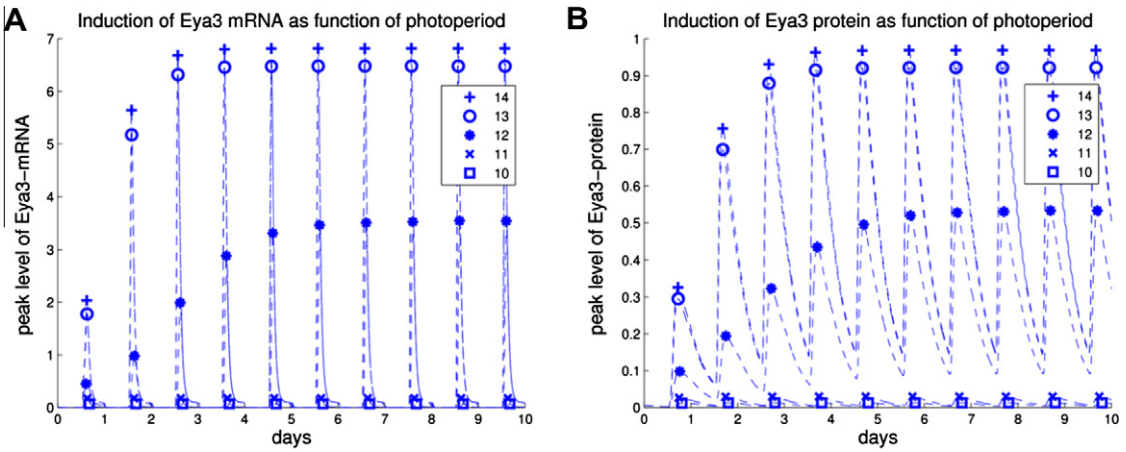

Fig. 5. Simulated Eya3 mRNA (A) and protein (B) induction. The simulated system was pre-adapted to short days (photoperiod 8 h) and at time 0 (dusk) transferred into longer days with photoperiods between 10 and 14 h. Symbols represent peak transcript and protein levels during one 24 h period. Parameters used for these simulations are given in Appendix A.

bute of members of the Eya gene family in other physiological contexts including eye development [13]. The predicted effect of direct or indirect EYA3 amplification is a transient increase in Eya3 mRNA and protein levels.

Fig. 5 displays the simulation results when the system was allowed to pre-adapt to short days (photoperiod 8 h) and thus establish a winter phenotype with low expression and protein levels of Eya3. At time 0, the system is exposed to longer photoperiods, where time 0 corresponds to the onset of the first night with reduced length. It can be seen that the induction of both mRNA (Fig. 5A) and protein (Fig. 5B) depend strongly on the photoperiod into which

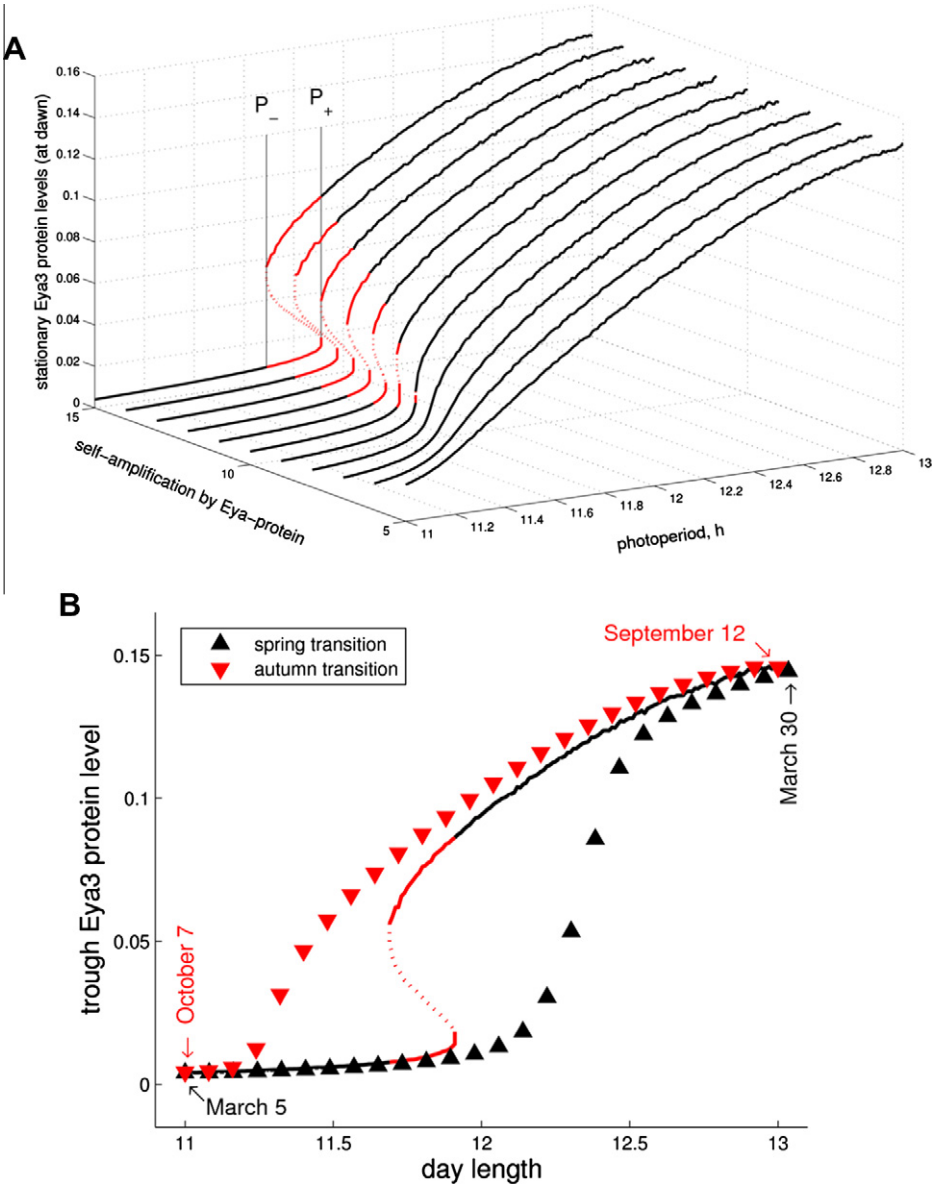

Fig. 6. Effect of Eya3 self-amplification on the ability to switch between summer and winter phenotype. A. Plots of stationary trough levels of EYA3 protein (z-axis) as function of photoperiod (x-axis) for different parameters f_E describing the factor by which EYA3 protein can induce Eya3 transcription (y-axis) (see Appendix A). For the different curves, only the factor f_E has been changed while the maximal level of Eya3 expression remained fixed. For low amplification values, protein levels change smoothly with increasing photoperiod. For high amplification values a range of photoperiods exists (red sections) in which there are three stationary protein levels. The unstable state is indicated by a dotted line. For these parameters and photoperiods the system is bistable, resulting in a hysteresis-like switching behavior between summer and winter phenotypes. The critical values P_+ and P_- at which the system undergoes a bifurcation are indicated for the largest investigated amplification value ($f_E = 15$). B. Simulations of Eya3 levels for changes in photoperiod as they are observed during spring (black symbols) and autumn (red) in Aberdeen, Scotland. In spring, day length increases from 11 h at March 5th to 13 h at March 30th with a daily increase of approximately 4 min 50sec. During autumn, day length shortens in a similar manner with a 13 h day at September 12th and an 11 h day at October 7th. The simulation results are presented as a phase-plot together with the numerically calculated hysteresis from Fig. 6A for $f_E = 15$. The parameter values are the same as in Appendix A, except $f_E = 15$.

the system was transferred. Whereas for photoperiods of less than 12 h no induction takes place and mRNA and protein levels remain low, transfer into photoperiods of more than 12 h leads to an increase in peak expression levels and concomitantly in protein levels throughout 3–4 days, after which EYA3 protein levels assume stable oscillations with a photoperiod-dependent amplitude. Thus, the mathematical model is able to reproduce one of the key physiological experiments characterising seasonal phenotypes, showing a similar pattern of Eya3 induction to that seen in the seasonal Soay sheep [8] (Fig. 3B).

Auto-activation of Eya3 expression is an important facet of the model to amplify and stabilise mRNA and protein levels. We therefore investigated how the factor by which Eya3 expression can be accelerated by its own protein (parameter f_E in Appendix A) influences the switching behavior between summer and winter phenotype. For this, we systematically varied the photoperiod between 11 and 13 h and numerically determined the resulting EYA3 protein levels. Since in a stable state adapted to a particular photoperiod Eya3 levels oscillate, we chose to describe the oscillations by a characteristic protein level at a certain time during the cycle. For this, we selected the trough levels, which are assumed immediately before the activation of Eya3 transcription and translation by the delayed clock signal ($\Delta\Psi$ after dusk). Thus, a stationary trough EYA3 protein level characterises a stable oscillation of EYA3 protein, which is assumed after adaptation to a particular photoperiod. This level is higher for stronger photoperiodic induction and therefore a suitable descriptor of the photoperiodic effect on EYA3 protein levels. A precise description of the numeric procedure for how the trough protein levels were determined is provided in Appendix B.

Fig. 6A displays the characteristic trough level of EYA3 protein as a function of the photoperiod for varying parameter f_E, which denotes the factor, by which Eya3 expression can be induced by EYA3 protein. For increasing factor f_E, a transition from a smooth change in protein concentrations to a switch-like behavior can be observed. For low amplification values, the protein concentrations change smoothly with photoperiod and for every value of the photoperiod one stationary state exists. This changes drastically as amplification values increase. Here, a range of photoperiods exists for which three stationary protein concentrations are found (red sections in Fig. 6A). The lower and upper values represent stable states while the middle value is an unstable state (dotted lines). Thus, the model system exhibits bistability and whether the low or the high expression level is reached depends on the initial conditions. For these parameter values, slow changes in daylength, as is observed under natural conditions, result in a hysteretic behavior (Fig. 6A and B). From winter to summer, EYA3 levels will follow the lower branch and only minimally increase until a critical photoperiod, P_+, is reached where the lower branch ceases to exist. As a consequence, a new state with high expression levels is assumed. From summer to winter, as days gradually become shorter, the system initially maintains high protein levels until the photoperiod drops below the critical value P_-, where the system again undergoes a bifurcation and assumes low expression values.

To explore the model behavior under gradual changes of the photoperiod, such as they are observed around spring and autumn equinox, we simulated the response to gradually increasing or decreasing day lengths. The results for actual day-length changes as they are observed in Aberdeen, Scotland (57°N) are depicted in Fig. 6B for a 25-day period in spring (black upward-pointing triangles) and a 25-day period in autumn (red downward-pointing triangles). To illustrate the switching behavior, these transitions are depicted as a phase plot together with the corresponding hysteresis from Fig. 6A (for $f_E = 15$). Thus, the spring transition proceeds from left to right (increasing day lengths), while the autumn transition proceeds from right to left (decreasing day lengths). Whereas in the considered period in spring (March 5–30th) the daily increase in photoperiod is almost linear, the protein levels of EYA3 exhibit a sharp increase between days 15 and 20, reflecting a switch from winter to summer phenotype. For the reverse transition in autumn, the transition is less pronounced, which can be explained by considering the shape of the hysteresis, where the upper branch displays a considerably steeper slope than the lower branch. Thus, the drop in protein concentration before the bifurcation point is reached is more pronounced than in the case of the spring transition. Nevertheless, a sharp drop can be observed at the bifurcation point around October 2nd–4th.

3. Conclusions

Since the work of Saunders et al. [2], the problem of how a circadian input generates a seasonal response has received limited attention in theoretical approaches. In a pioneering theoretical work, Pittendrigh and Daan [14] developed a mathematical model that is based on the assumption that two oscillators with different entrainment properties coexist to explain changes in the activity patterns in nocturnal animals after exposure to different light regimes. Schaap et al. [15] have developed a mathematical model to describe how neurons in the suprachiasmatic nucleus (SCN) in rats respond to different photoperiods. While these models are certainly important for our understanding of molecular mechanisms triggered by photoperiodic changes, they do not address the question how seasonal phenotypes are induced by changes in photoperiod. We have provided a mathematical model describing exactly this transition from a light-dependent input to a seasonal expression pattern of an output gene. While the model is still rather simple, it nevertheless elucidates the principles behind this process and we therefore believe it can serve as a theoretical framework in which new experimental observations of seasonal responses can be interpreted.

A key mechanism to generate stable expression patterns for different photoperiods is the positive feedback of the EYA3 protein on the transcription rates of the Eya3 gene. While it is not clear whether the molecular mechanism is indeed a direct activation of the gene expression by the protein itself or whether a more indirect positive feedback operates (for example via TSH effects in TSH producing cells of the PT, which appear to

express TSH receptors as well as melatonin receptors [16,17]), we could demonstrate that in principle this mechanism is capable of producing a switch between summer and winter phenotypes induced by gradual changes in day-length. In other words, while a circadian clock based coincidence timer mechanism can produce a graded amplitude response to the gradient of photoperiod, additional mechanisms appear to be required to produce the behaviour seen in nature.

An interesting feature of the amplifier model is the hysteresis it predicts. Exploration of this property requires experimental data from short to long day transitions and *vice versa*, which are very sparse in the literature. Nevertheless, one study has reported that downstream changes in brain biology in hamsters exposed to declining daylength follow dynamics distinct from those predicted from data on increasing daylength, possibly consistent with hysteresis [18]. Perhaps consonantly, our own studies of Eya3 RNA expression in sheep (DH unpublished observations) show that expression patterns are highly sensitive to photoperiodic history. An interesting question is whether an imminent switch between summer and winter phenotypes can in principle be anticipated by experimental measurements. The theoretical work by Scheffer and colleagues [19] suggests that prior to a critical transition caused by a saddle-node bifurcation (as is the case in our model during a switch between the two states), fluctuation of the key variables should be significantly increased due to the phenomenon of critical slowing down [19]. In principle, this should be manifest in increased variance in Eya3 (or possibly TSH) expression levels as animals approach the critical photoperiodic state transition. Extant data are insufficient to test this prediction, and further RNA profiling work would be required.

The issue of producing transitions from graded input signals has also been addressed in developmental biology, notably in the question of body segmentation. Here a clock and wave-front model has gained acceptance as a means to account for the formation of regularly repeating body segments [20], while the issue of how discontinuous boundaries form between structures has been less clear. Recent modelling work on this issue suggests that mutually repressive regulatory interactions between retinoic acid and fibroblast growth factor signalling are crucial to boundary formation in this system. Coupled mutual repression generates bistability remarkably similar to that predicted in our analysis of the photoperiodic response [21]. The analogy between seasonal photoperiodic switching and developmental biology is suggested more generally by the central role played by Eya3 in the photoperiodic response. Eya3 has previously been considered as part of the developmental switching involved in eye, pituitary and limb development [13], and has only recently been appreciated for it role in seasonal timing [8,9]. Histogenesis-based phenomena have recently been proposed to underlie innate long-term timing of seasonal transitions in biology [22]. We conclude that modelling and lab-based approaches that explicitly recognise the developmental properties of seasonal timers will be productive avenues for further study.

Acknowledgments

This work was supported by the Biotechnology and Biological Sciences Research Council, UK, and the Scottish Funding Council through the Scottish Life Sciences Alliance (SULSA).

Appendix A. Mathematical formulation of the model

The model equations given below reflect the interactions described in the text above. The model contains four variables. Cry mRNA (C) and CRY protein (P) form the coincidence timer module, which translates the photoperiodic input into a gated output, leading to a photoperiod-dependent transcriptional activity of Eya3. The feedback amplification module consists of Eya3 mRNA (X) and EYA3 protein (E).

The external light conditions are sensed by melatonin which is described by a time-dependent step function $M(t)$ which equals 1 in darkness and 0 in light.

The differential equations read

$$\dot{C} = k_C \cdot M(t) \frac{1}{1 + \left(\frac{P}{I_P}\right)^{n_C}} - d_C \cdot C \tag{1}$$

$$\dot{P} = k_P \cdot C - d_P \cdot P \frac{1}{1 + \left(\frac{M(t)}{I_M}\right)^{n_P}} \tag{2}$$

$$\dot{X} = k_X \cdot C(t - \Delta\Psi) \cdot \frac{1}{1 + \left(\frac{P}{I_{MX}}\right)^{n_X}} \cdot \left[1 + (f_E - 1) \cdot \frac{E^{n_{AE}}}{K_{AE}^{n_{AE}} + E^{n_{AE}}}\right] - d_X \cdot X \tag{3}$$

$$\dot{E} = k_E \cdot X - d_E \cdot E \tag{4}$$

The first term in Eq. (1) reflects activation of Cry transcription by melatonin and inhibition by CRY protein, the degradation is assumed to follow first-order kinetics. CRY protein production – see Eq. (2) – is assumed to be proportional to its mRNA and the degradation is inhibited by melatonin. Eq. (3) contains the gating mechanism through the coincidence timer. As described above, we assume that a gene exists which peaks in a phase-locked manner at a fixed time after the peak of Cry. We use Cry mRNA as an indicator of the phase of the clock and let the transcription of Eya3 mRNA (X) be induced with a fixed time delay. This is expressed in the term $C(t - \Delta\Psi)$. Further, Cry protein is inhibiting transcription and EYA3 protein (E) can accelerate transcription. The factor f_E describes the extent by which the transcription can be maximally enhanced through EYA3 protein.

The following parameters were assumed for most of the simulations.

Production rate constants (units concentration/h): $k_C = 2$, $k_P = 0.5$, $k_X = 2.5$, $k_E = 0.08$.

Degradation rate constants (1/h): $d_C = d_P = 1$, $d_X = 3$, $d_E = 0.1$.

Inhibition constants (conc.): $I_P = 0.25$, $I_M = I_{MX} = 0.2$.

Activation constant (conc.): $K_{AE} = 0.1$.

Hill coefficients: $n_C = n_P = n_X = 4$, $n_{AE} = 3$.

Activation factor: $f_E = 10$.
Time delay: $\Delta\Psi = 12.5$ h.

Appendix B. Determination of stable trough EYA3 protein levels

The stable EYA3 protein oscillations are characterized by a value at a fixed time ($\Delta\Psi$) after the onset of dark. These are close to the minimal values during a diurnal cycle, because at this time the delayed induction of Eya3 mRNA production by Cry begins and Eya3 mRNA levels and EYA3 protein levels begin to rise. Since degradation of EYA3 protein is proportional to the protein level itself (Eq. (4)), trough levels are a monotonous function of the oscillatory amplitude and thus serve as a unique characterization of the stable EYA3 protein oscillations.

For Fig. 6A, these stationary trough levels have been systematically determined for different photoperiods and amplification factors f_E in the following way: The photoperiod was systematically varied between 11 h and 13 h with a step size of 0.01 h and the amplification factor f_E was varied between 5 and 15 in steps of 1. Because the maximally possible Eya3 transcription rate is $k_X \cdot f_E$, the base rate of Eya3 transcription, k_X, was simultaneously adjusted to $k_X = 25/f_E$. Thus, the maximal transcription rate is identical for all values of f_E.

Numeric integration of the equation system (1)–(4) over a 24 h our period allows to determine the absolute daily change of Eya3 protein, ΔP, in dependence on the trough protein level, P_0, which is assumed at dusk+$\Delta\Psi$. However, in addition to initial values, the integration of a delay differential equation requires knowledge of the history of the system. In this particular system, the history can easily be determined, exploiting that C is the only variable with delay and the differential equations for P and C do not depend on the other variables, X and E: Eqs. (1) and (2) are integrated for a sufficiently long time (we used 20 days) until the stable oscillations have been closely approximated, and the result is used as the history for the integration of the full system. This procedure allows defining a function $\Delta P = \Delta P(P_0)$, of which the zeroes have been determined numerically for each combination of photoperiod and amplification factor f_E.

References

[1] Goldman B. Circannual rhythms and photoperiodism. In: Dunlap JC, Loros JL, DeCoursey PJ, editors. Chronobiology – biological timekeeping. Massachusetts: Sinauer Asscoiates; 2004.
[2] Saunders DS. Erwin Bünning and Tony Lees, two giants of chronobiology and the problem of time measurement in insect photoperiodism. J Insect Physiol 2005;51:599–608.
[3] Elliott JA. Circadian rhythms and photoperiodic time measurement in mammals. Fed Proc 1976;35:2339–46.
[4] Hazlerigg DG, Loudon ASI. New insight sinto ancient seasonal life timers. Curr Biol 2008;18:R795–804.
[5] Krol E et al. Strong pituitary and hypothalamic responses to photoperiod but not to 6-methoxy-2-benzoxazolinone in female common voles (*Microtus arvalis*). Gen Comp Endo 2012;179:289–95.
[6] Takahashi JS et al. The genetics of mammalian circadian order and disorder: implications for physiology and disease. Nat Rev Genet 2008;9:764–75.
[7] Ueda HR et al. System-level identification of transcriptional circuits underlying mammalian circadian clocks. Nat Genet 2005;37:187–92.
[8] Dardente H et al. A Molecular switch for photoperiod responsiveness in mammals. Curr Biol 2010;20:2193–8.
[9] Masumoto K-h et al. Acute induction of Eya3 by late-night light triggers TSHb expression in photoperiodism. Curr Biol 2010;20:2199–206.
[10] Johnston JD et al. Multiple effects of melatonin on rhythmic clock gene expression in the mammalian pars tuberalis. Endocrinology 2006;147:959–65.
[11] Lai K et al. The sonic hedgehog signalling system as a bistable genetic switch. Biophys J 2004;86:2748–57.
[12] Wilhelm T. The smallest chemical reaction system with bistability. BMC Systems Biol 2009;3:90.
[13] Rebay I et al. New vision from eyes absent: transcription factors as enzymes. T I G 2005;21:163–71.
[14] Pittendrigh CS, Daan S. A functional analysis of circadian pacemakers in nocturnal rodents. V. Pacemaker structure: a clock for all seasons. J Comp Physiol 1976;106:333–55.
[15] Schaap J et al. Heterogeneity of rhythmic suprachiasmatic nucleus neurons: implications for circadian waveform and photoperiodic encoding. Proc Natl Acad Sci USA 2003;100:15994–9.
[16] Hanon E et al. Ancestral TSH mechanism signals summer in a seasonal mammal. Curr Biol 2008;18:1147–52.
[17] Ono H et al. Involvement of thyrotrophin in photoperiodic signal transduction in mice. Proc Natl Acad Sci USA 2008;105:18238–42.
[18] Yasuo S et al. Photoperiodic control of TSH- beta expression in the mammalian pars tuberalis has different impacts on the induction and suppression of the hypothalamo-hypopysial gonadal axis. J Neuroendocrinol 2010;22:43–50.
[19] Scheffer M et al. Early warning signals for critical transitions. Nature 2009;461:53–9.
[20] Cooke J, Zeeman EC. A clock and wavefront model for control of the number of repeated structures during animal morphogenesis. J Theor Biol 1976;58:455–76.
[21] Goldbeter A et al. Sharp developmental thresholds defined through bistability by antagonistic gradients of retinoic acid and FGF signalling. Dev Dyn 2007;236:1495–508.
[22] Hazlerigg DG, Lincoln GA. Hypothesis: cyclical histogenesis is the basis of circannual timing. J Biol Rhythms 2011;26:471–85.